New Autoinducing Peptides Regulate Antibiotic Production for Sculpting Microbiome

Nanzhu Chen[1†], Peiyan Cai[1†], Xiaoqian Lin[1†], Zhi-Man Song[1], Jiaze He[1], Zewen Li[2], Zhuohan Li[1], Dengwei Zhang[1], Yi Song[2]* & Yong-Xin Li[1]*

[1] Department of Chemistry, The University of Hong Kong, Pokfulam Road, Hong Kong, China

[2] Shenzhen Key Laboratory of Plant Genetic Engineering and Molecular Design, Institute of Plant and Food Science, Department of Biology, School of Life Sciences, Southern University of Science and Technology, Shenzhen, China.

†: These authors contributed equally to this work: Nanzhu Chen, Peiyan Cai, Xiaoqian Lin

*: To whom correspondence may be addressed.

Email: yxpli@hku.hk & songy3@sustech.edu.cn.

Supplementary figures

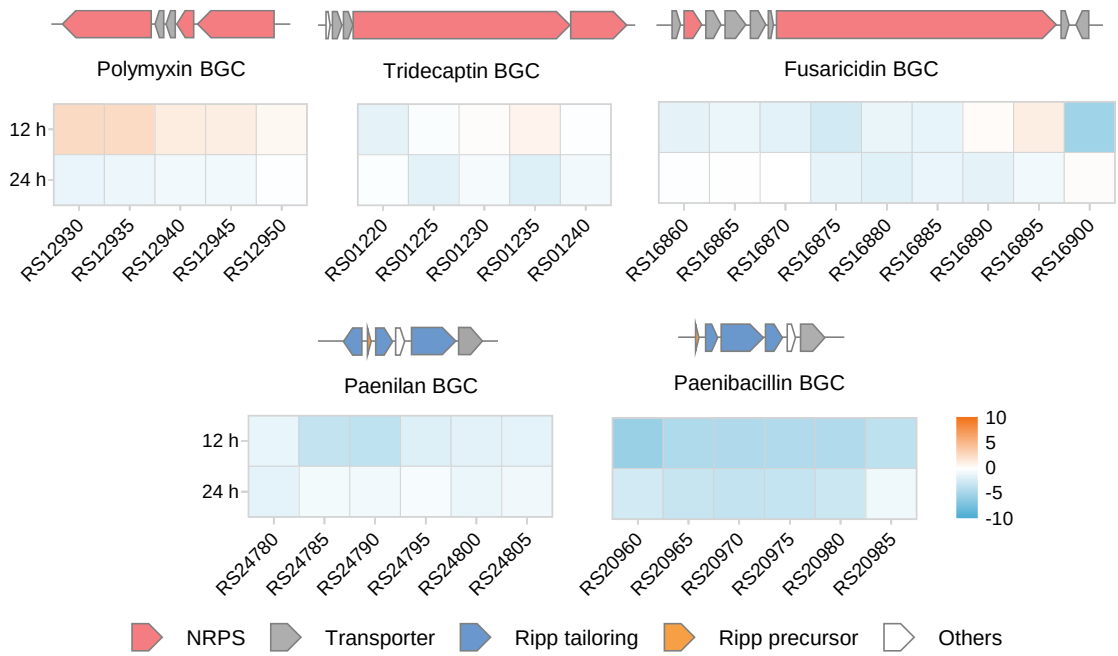

Figure S1. The BGC expression of known compounds in *P. polymyxa* Δ*CAR* strain relative to WT strain.

The heatmaps display the $\log_2$ fold change. The diagrams depicting the corresponding genes are shown below.

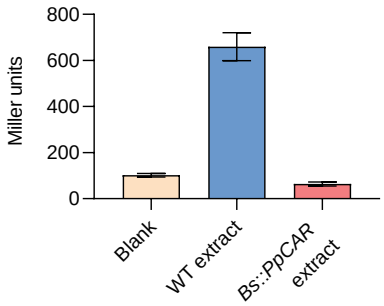

Figure S2. The lacZ activities of reporter strain *P. polymyxa*-Ppae-lacZ in addition of the *B. subtilis* JH642::*PpCAR* extract.

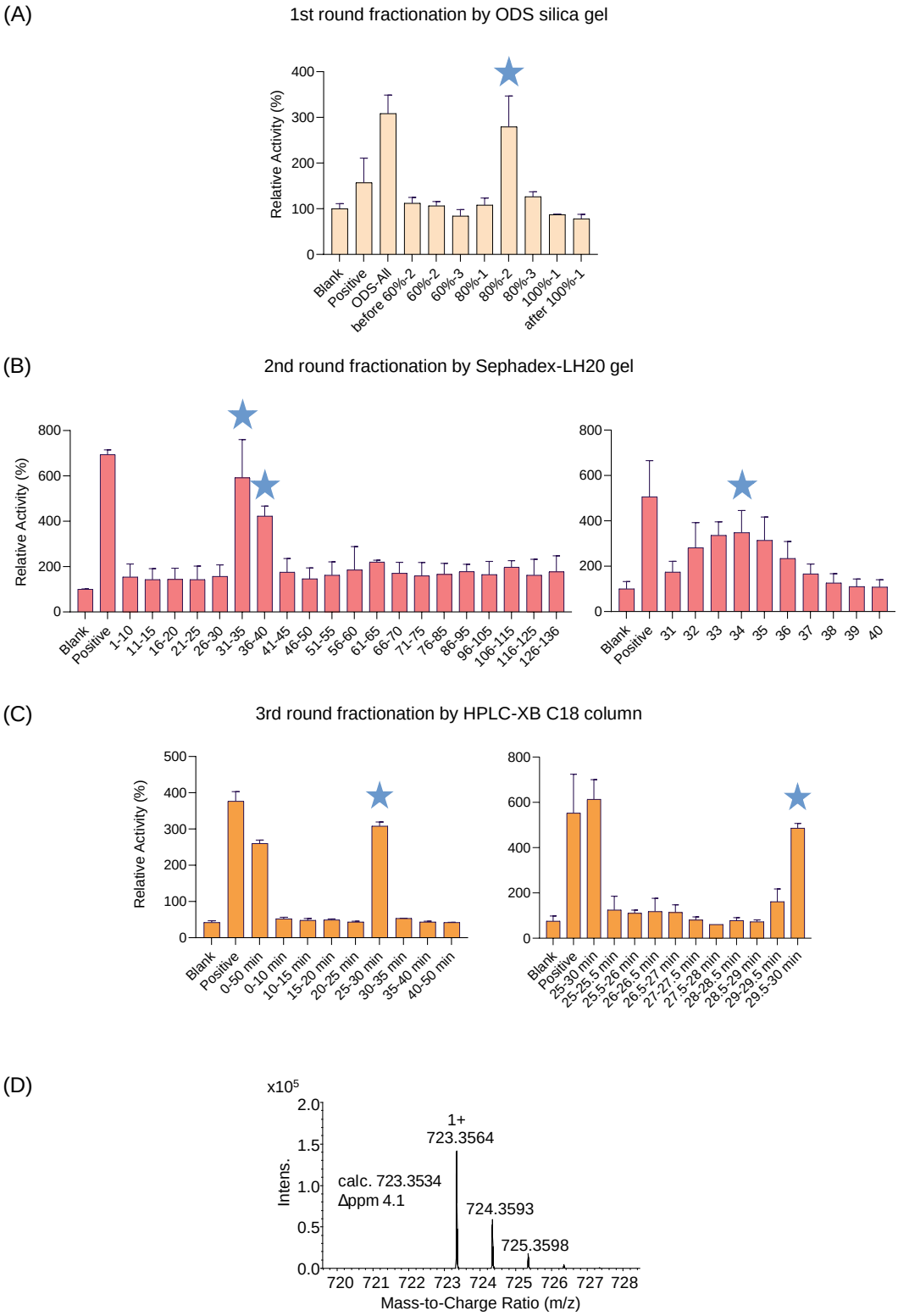

Figure S3. The lacZ activities of reporter strain *P. polymyxa*-Ppae-lacZ under each fraction from *P. polymyxa* ATCC 842 culture crude extracts.

(A) The WT extract fermentation was fractionated by ODS silica gel open column, and the lacZ activities of the reporter strain under each fraction were analyzed.

(B) The sample 80%-2 from (A) was further fractionated by Sephadex-LH20 gel open column. Every

5 fractions were mixed into one sample for bioactivity screening (left figure). Within samples 31-40, each single fraction was subjected to bioactivity screening (right figure).
(C) The sample 34 from (B) was further fractionated by HPLC with XB C18 column. Fractions in every 5 minutes were collected for bioactivity screening (left figure). Within 25 to 30 min, fractions were collected every 30 seconds for bioactivity screening (right figure).
(D) The mass spectrum of compound in fraction 29.5 to 30 min in (C).

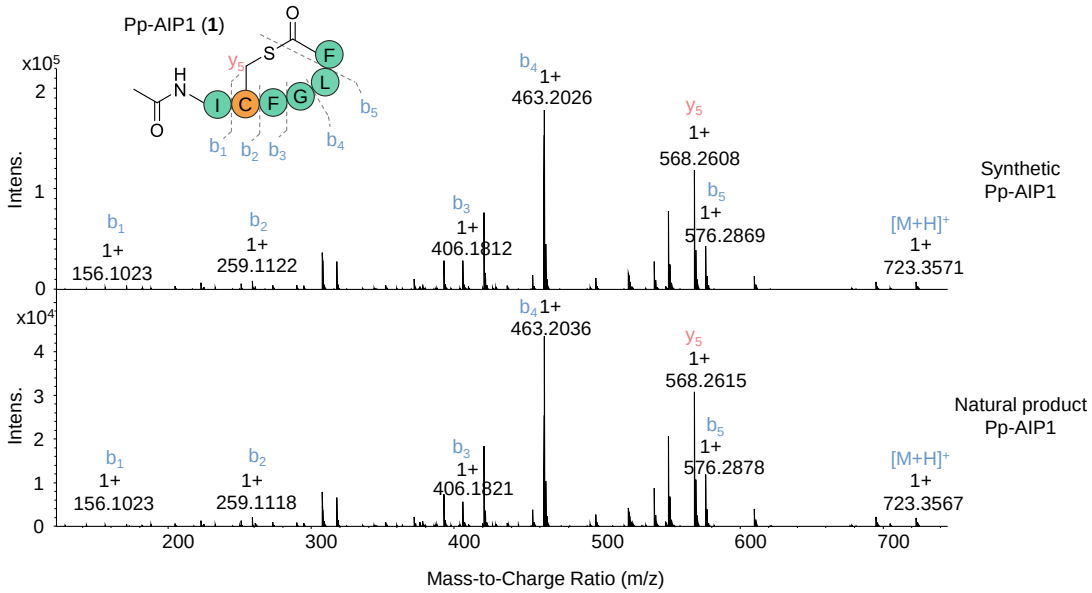

Ion	Sequence	Formula	Calculated Mass Value	Exact Mass Value (Natural Product)	PPM	Exact Mass Value (Chemical Synthesis)	PPM
parent mass	Ac-I-[CFGLF]	$C_{37}H_{51}N_6O_7S^+$	723.3534	723.3567	4.56	723.3571	5.12
b5	Ac-ICFGL	$C_{28}H_{42}N_5O_6S^+$	576.2850	576.2878	4.86	576.2869	3.30
b4	Ac-ICFG	$C_{22}H_{31}N_4O_5S^+$	463.2010	463.2036	5.61	463.2026	3.45
b3	Ac-ICF	$C_{20}H_{28}N_3O_4S^+$	406.1795	406.1821	6.40	406.1812	4.19
b2	Ac-IC	$C_{11}H_{19}N_2O_3S^+$	259.1111	259.1118	2.70	259.1122	4.25
b1	Ac-I	$C_8H_{14}NO_2^+$	156.1019	156.1023	2.56	156.1023	2.56
y5	[CFGLF]	$C_{29}H_{38}N_5O_5S^+$	568.2588	568.2615	4.75	568.2608	3.52

Figure S4. HR-MS/MS analysis of identified signaling molecule (natural product) Pp-AIP1 and synthetic Pp-AIP1.

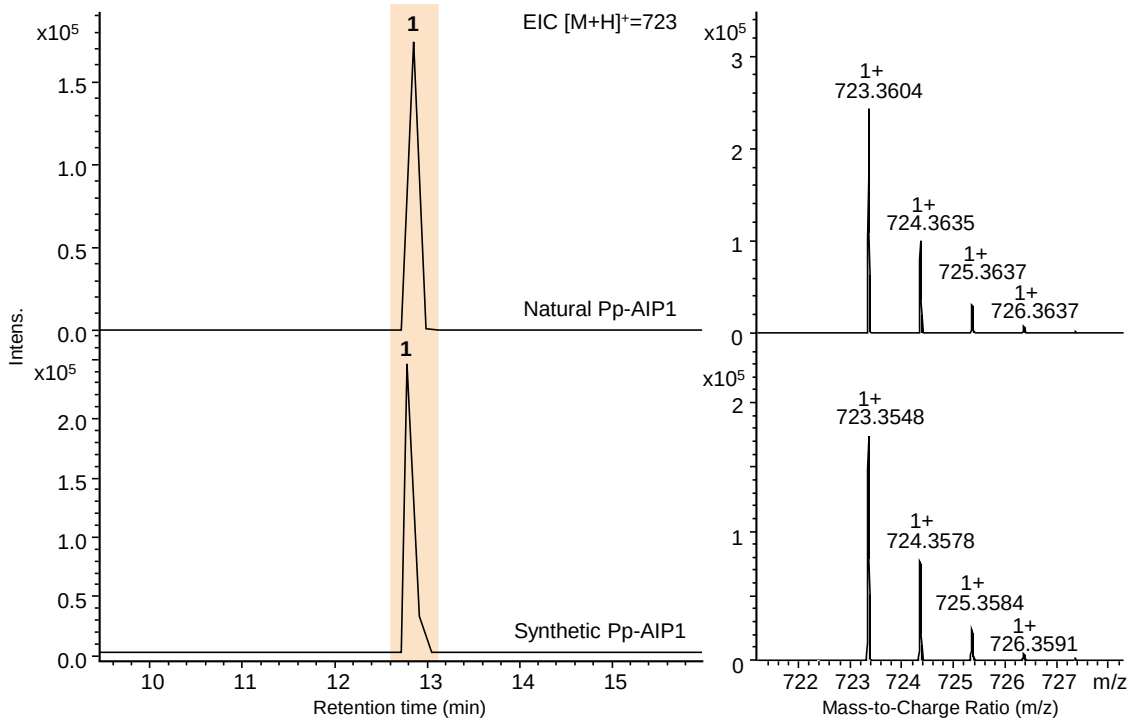

Figure S5. Comparison by UPLC-HRMS of retention time and mass spectrum of natural product Pp-AIP1 with synthetic Pp-AIP1.

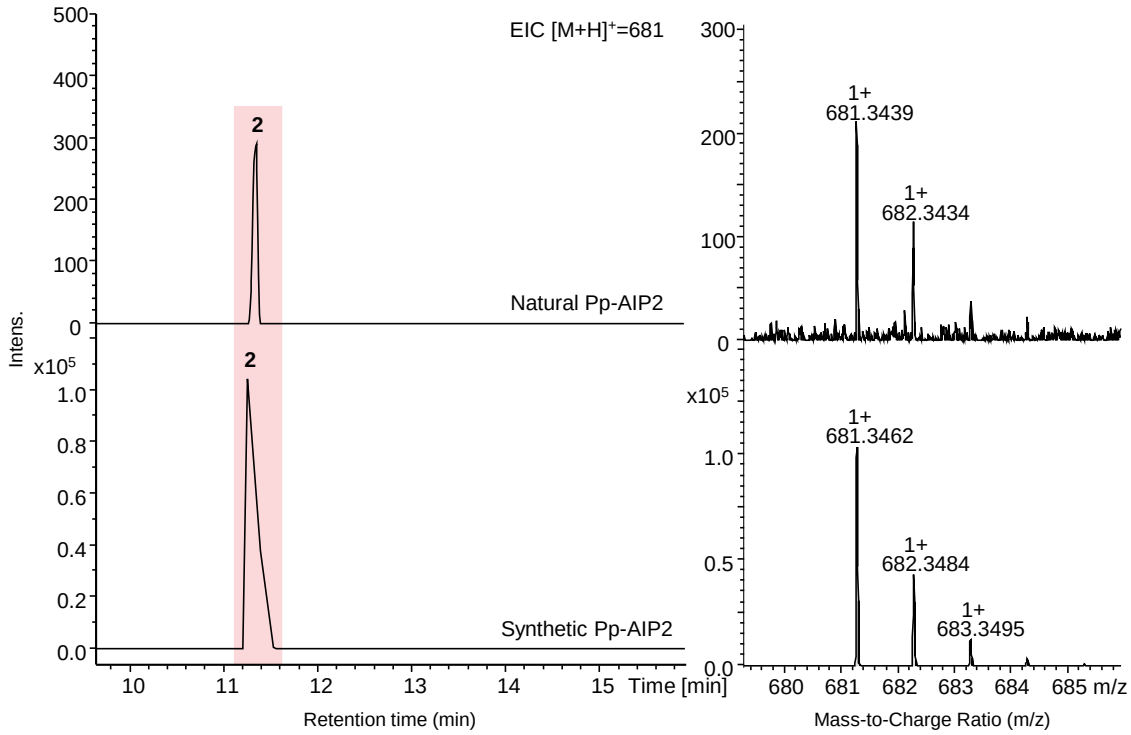

Figure S6. Comparison by UPLC-HRMS of retention time and mass spectrum of natural product Pp-AIP2 with synthetic Pp-AIP2.

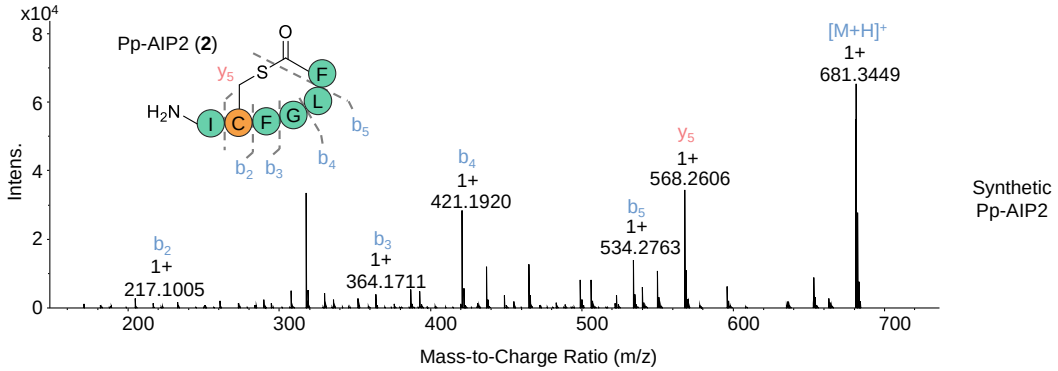

Ion	Sequence	Formula	Calculated Mass Value	Exact Mass Value (Chemical Synthesis)	PPM
parent mass	I-[CFGLF]	$C_{35}H_{49}N_6O_6S^+$	681.3429	681.3449	2.94
b5	ICFGL	$C_{26}H_{40}N_5O_5S^+$	534.2745	534.2763	3.37
b4	ICFG	$C_{20}H_{29}N_4O_4S^+$	421.1904	421.1920	3.80
b3	ICF	$C_{18}H_{26}N_3O_3S^+$	364.1689	364.1711	6.04
b2	IC	$C_9H_{17}N_2O_2S^+$	217.1005	217.1009	1.84
y5	[CFGLF]	$C_{29}H_{38}N_5O_5S^+$	568.2588	568.2606	3.17

Figure S7. HR-MS/MS analysis of synthetic Pp-AIP2.

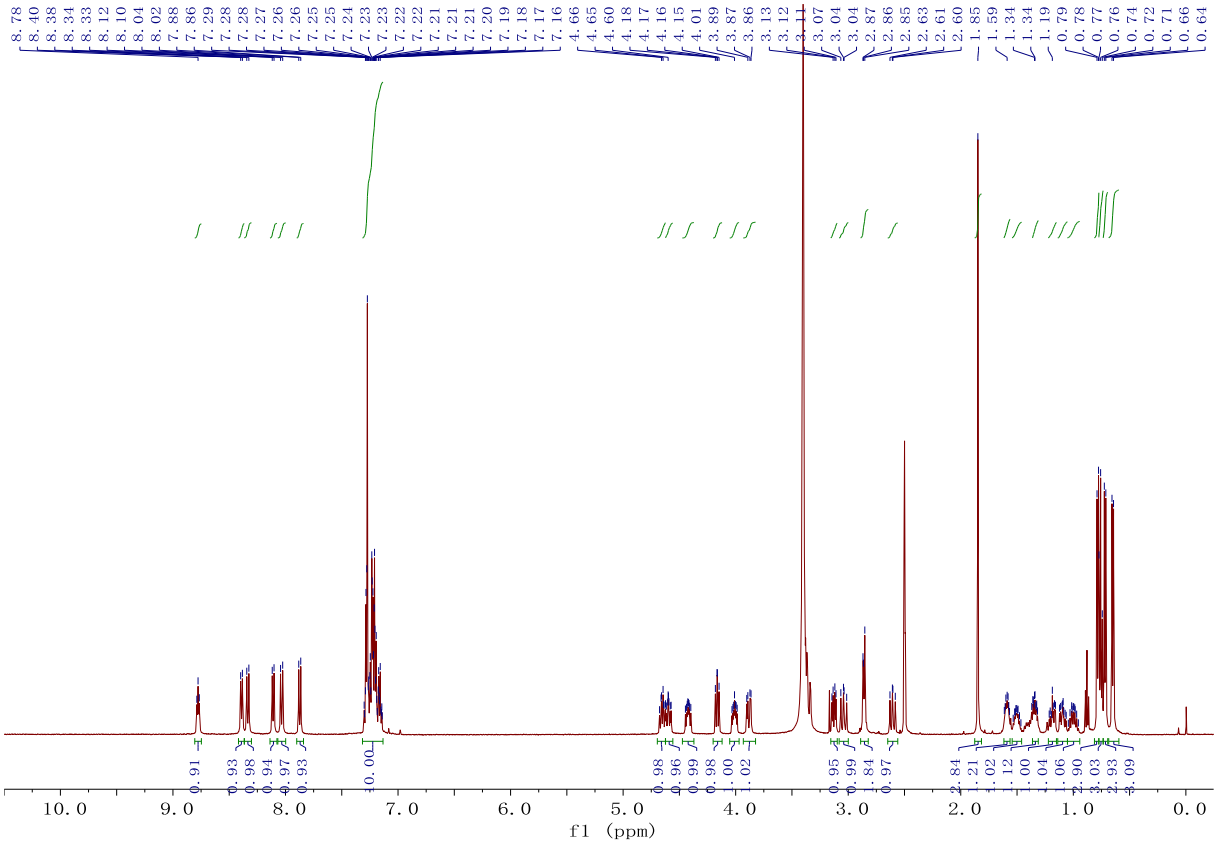

Figure S8. [1]H NMR spectrum of Pp-AIP1 (**1**) (600 MHz, DMSO-d_6).

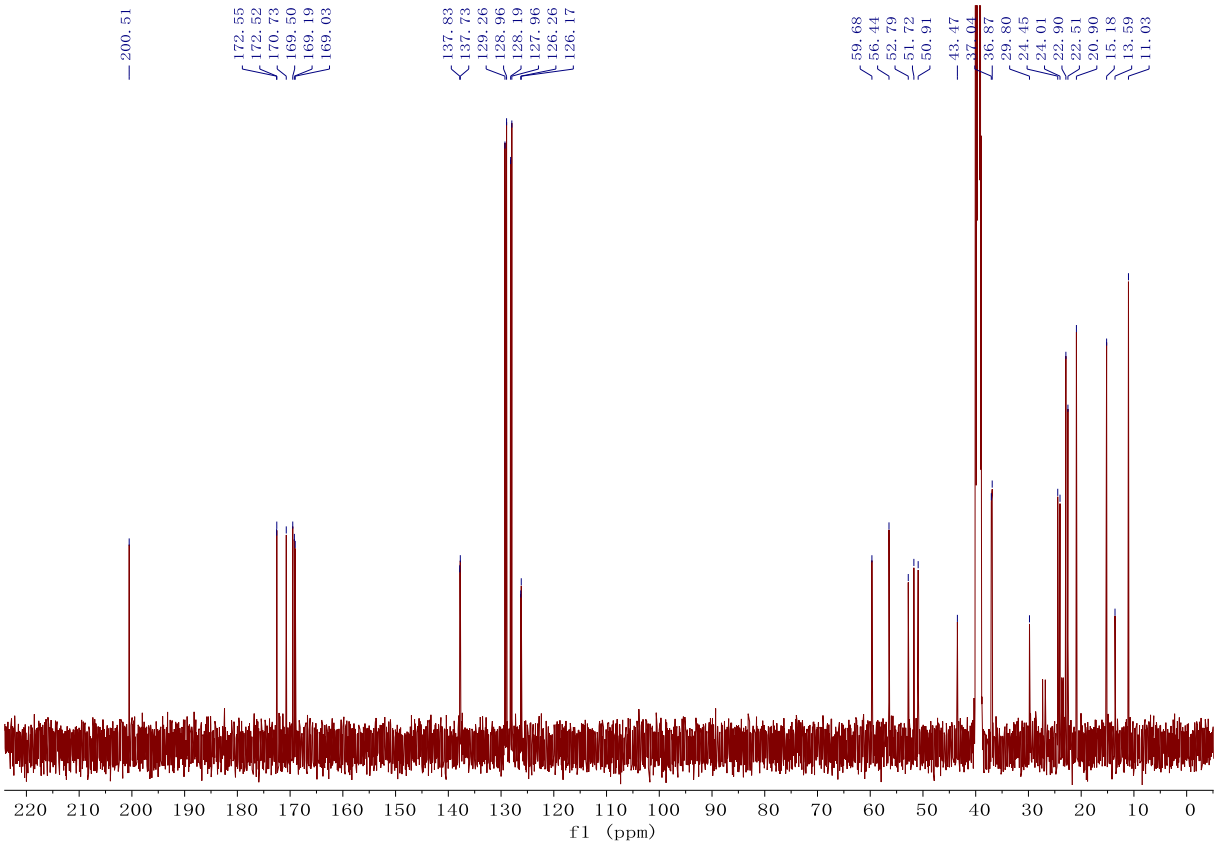

Figure S9. [13]C NMR spectrum of Pp-AIP1 (**1**) (150 MHz, DMSO-d_6).

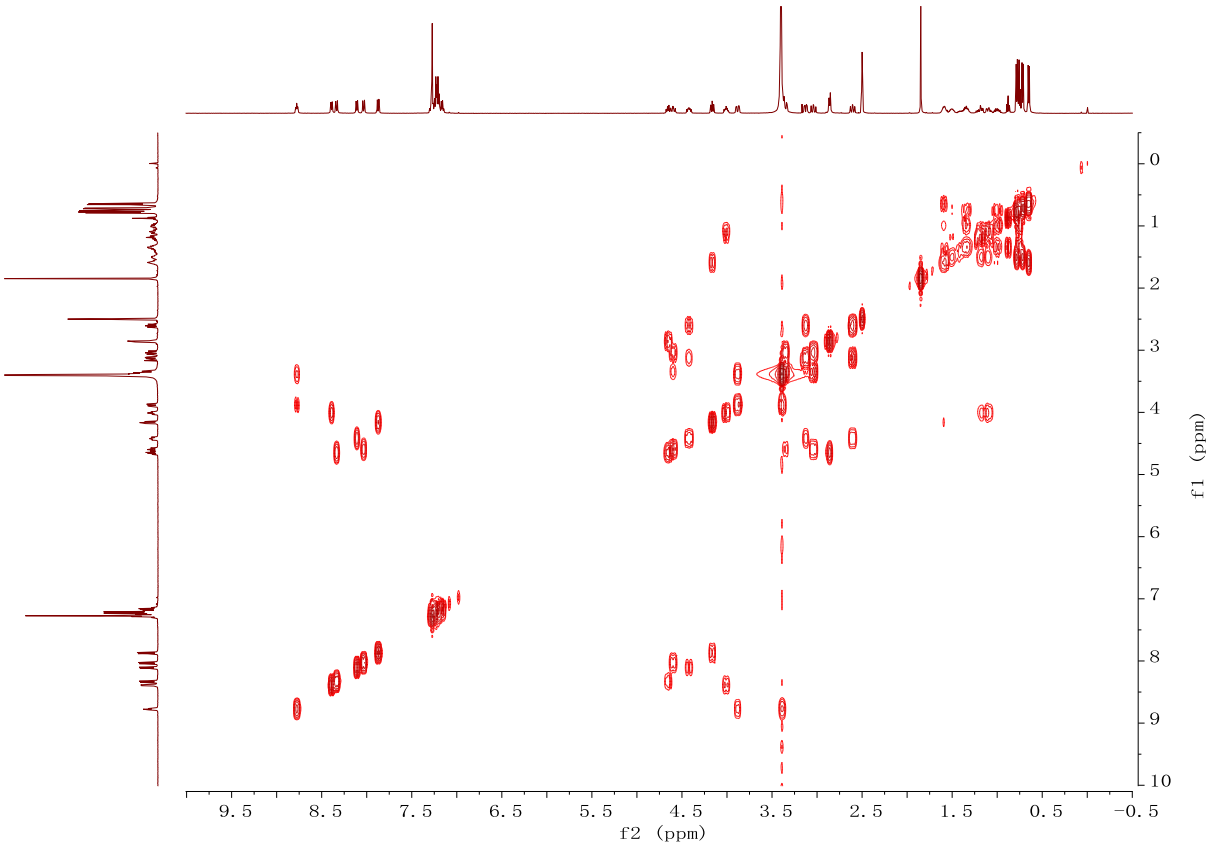

Figure S10. ^{1}H-^{1}H COSY NMR spectrum of Pp-AIP1 (**1**) (600 MHz, DMSO-d_6).

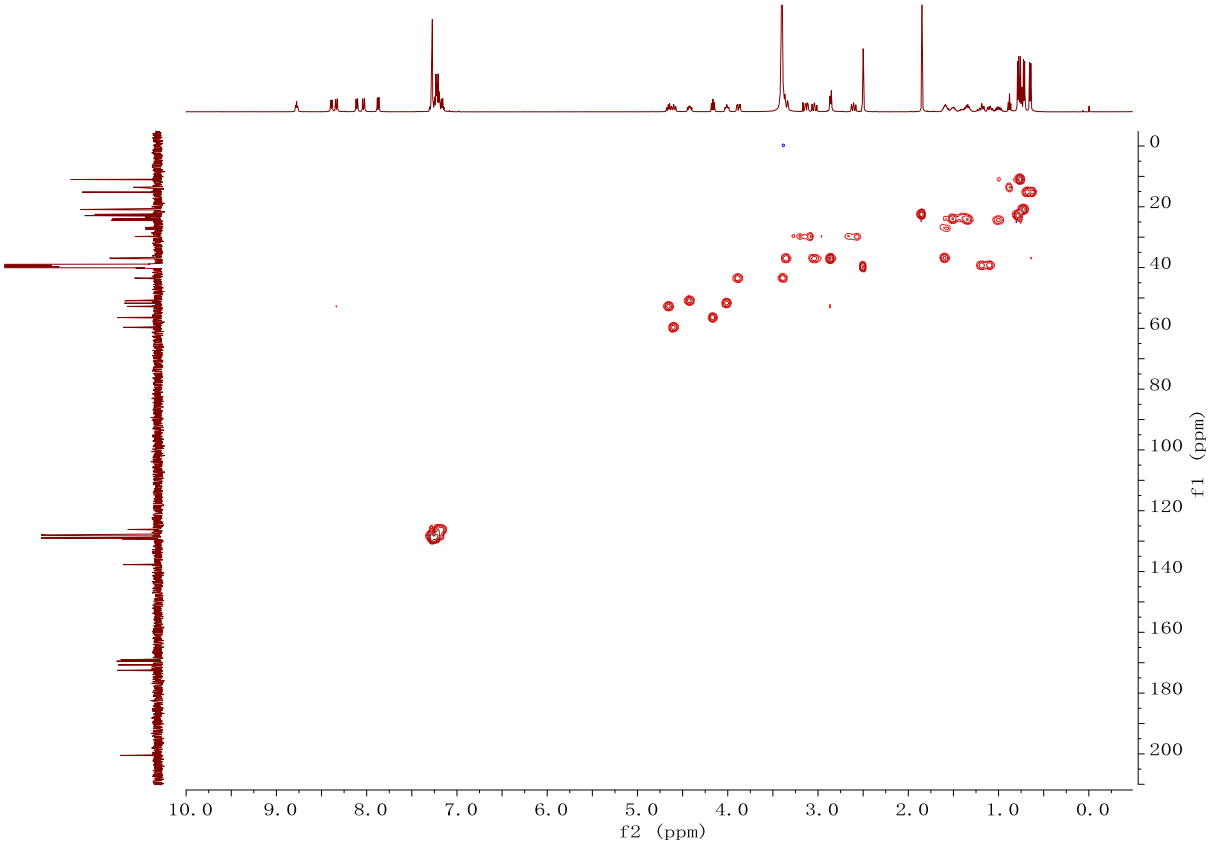

Figure S11. HSQC NMR spectrum of Pp-AIP1 (**1**) (600 MHz, DMSO-d_6).

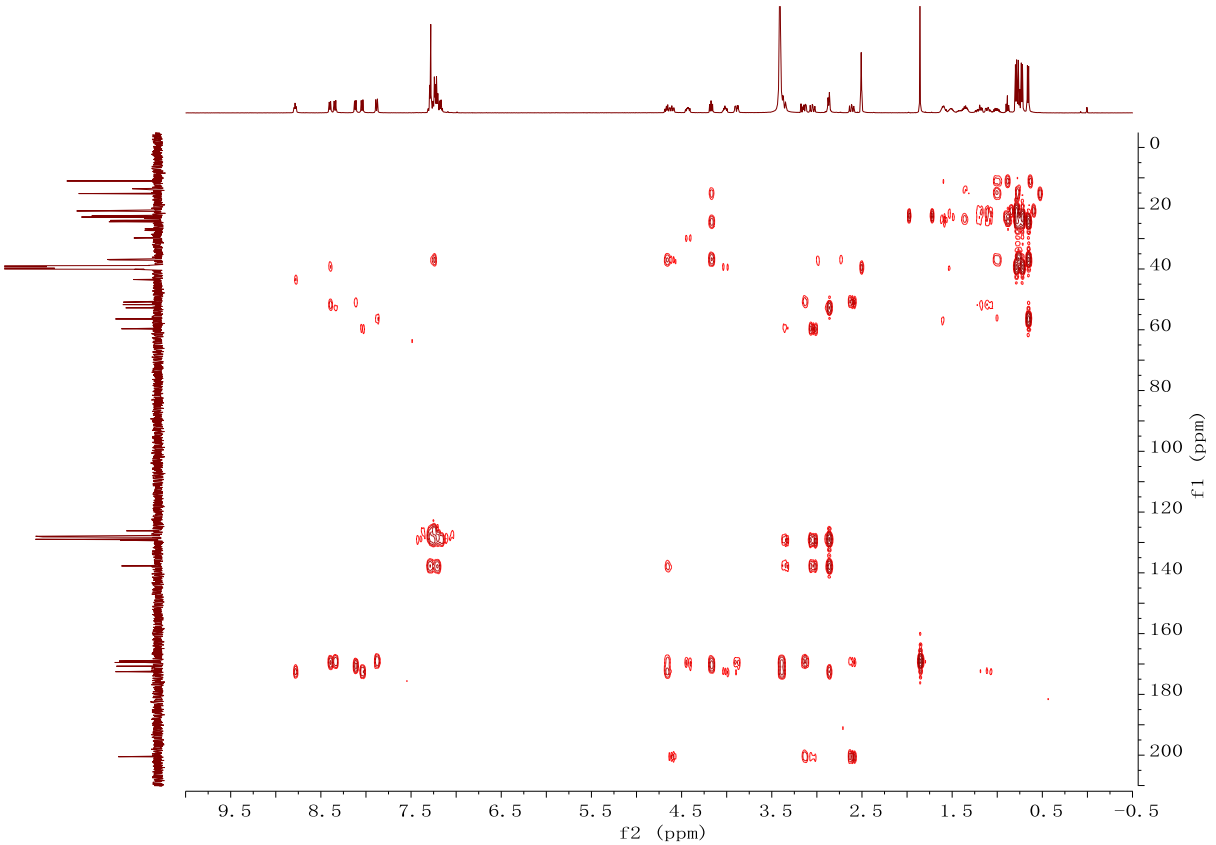

Figure S12. HMBC NMR spectrum of Pp-AIP1 (**1**) (600 MHz, DMSO-d_6).

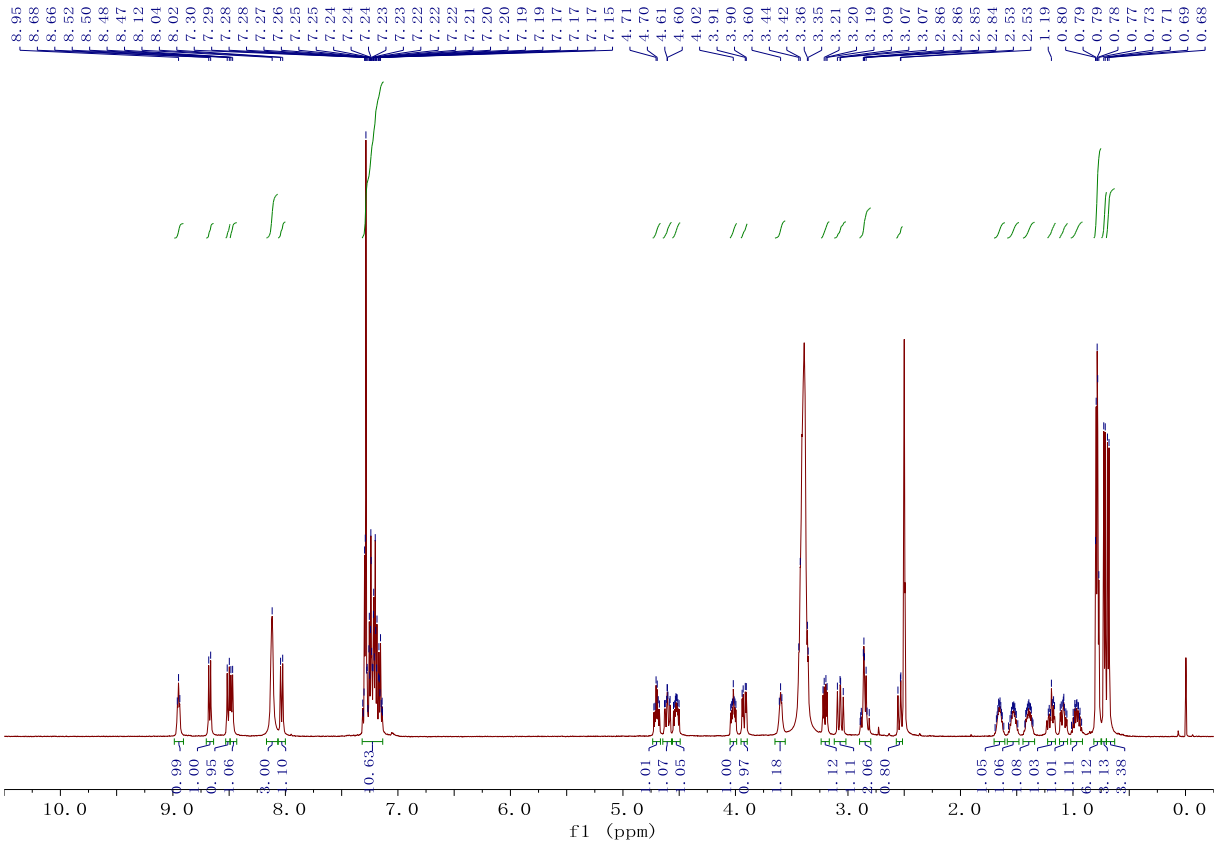

Figure S13. ^{1}H NMR spectrum of Pp-AIP2 (**2**) (600 MHz, DMSO-d_6).

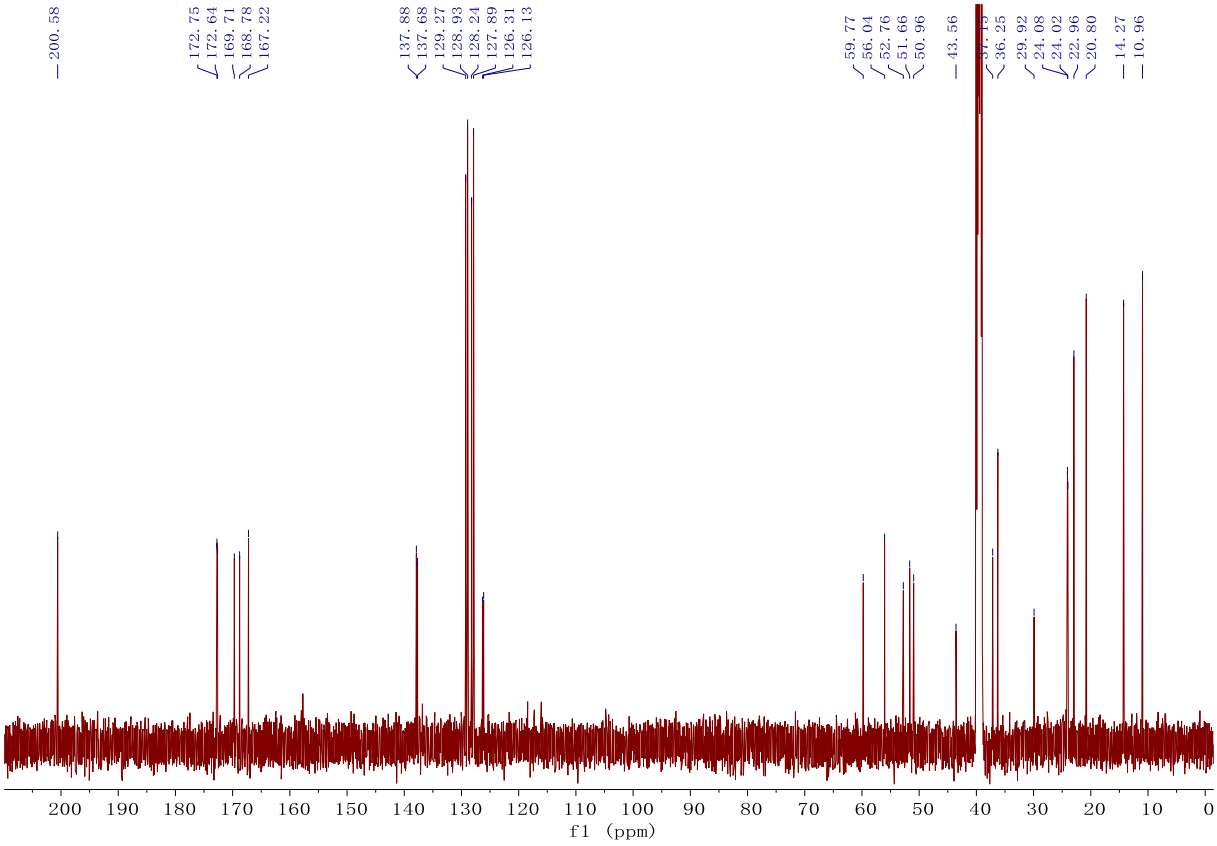

Figure S14. ^{13}C NMR spectrum of Pp-AIP2 (**2**) (150 MHz, DMSO-d_6).

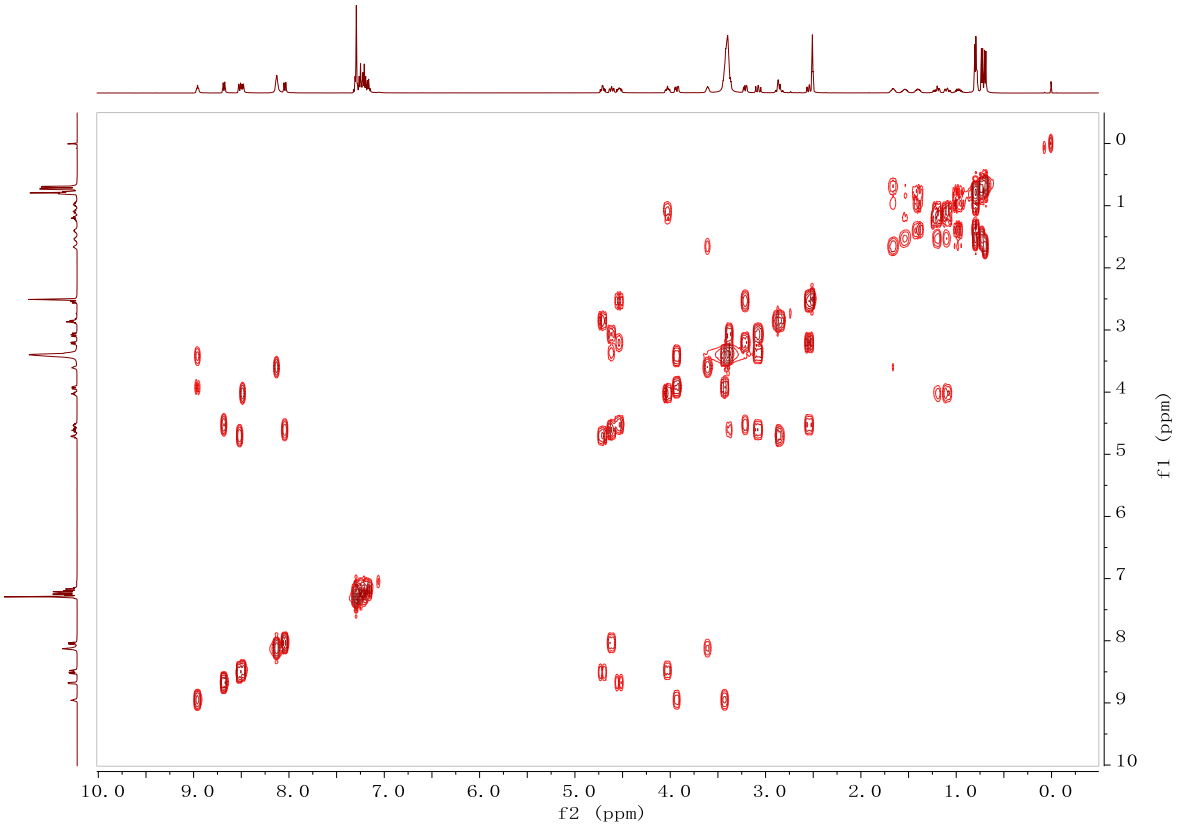

Figure S15. ^{1}H-^{1}H COSY NMR spectrum of Pp-AIP2 (**2**) (600 MHz, DMSO-d_6).

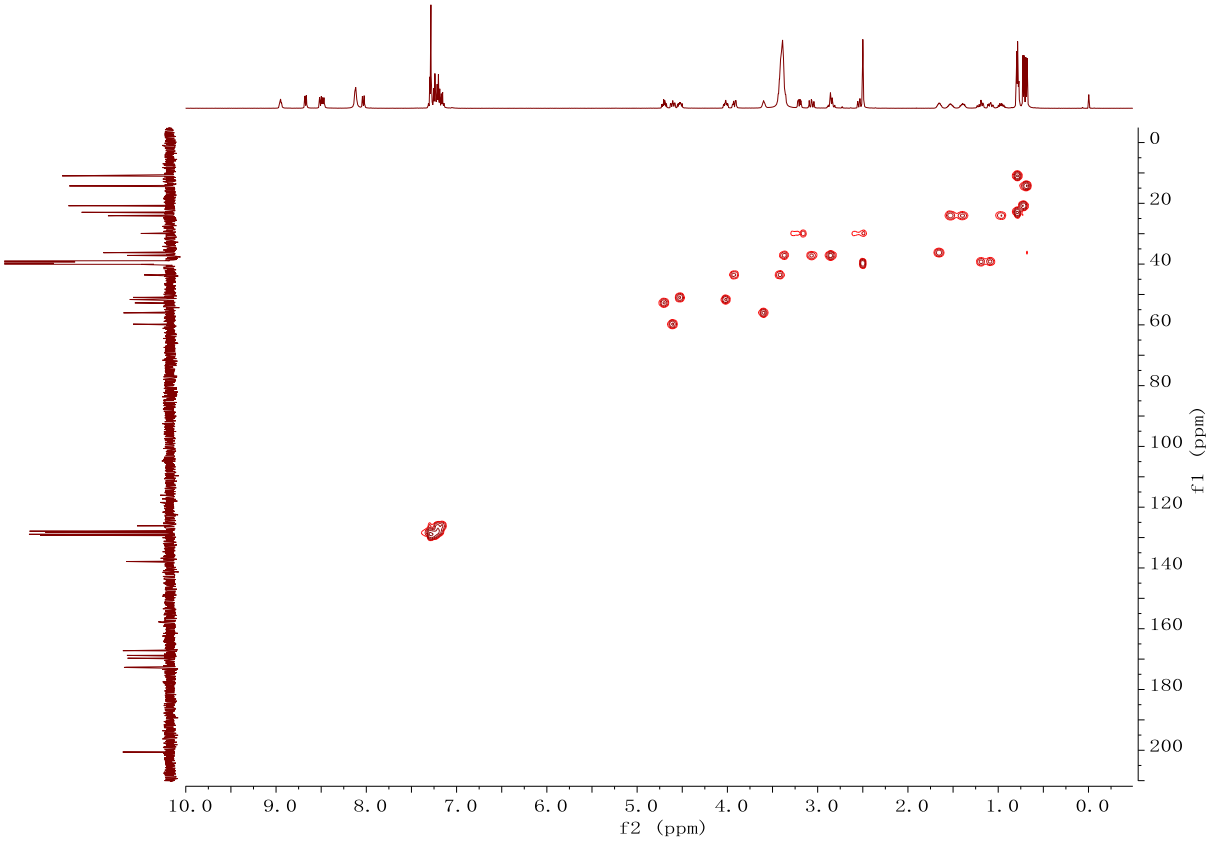

Figure S16. HSQC NMR spectrum of Pp-AIP2 (**2**) (600 MHz, DMSO-d_6).

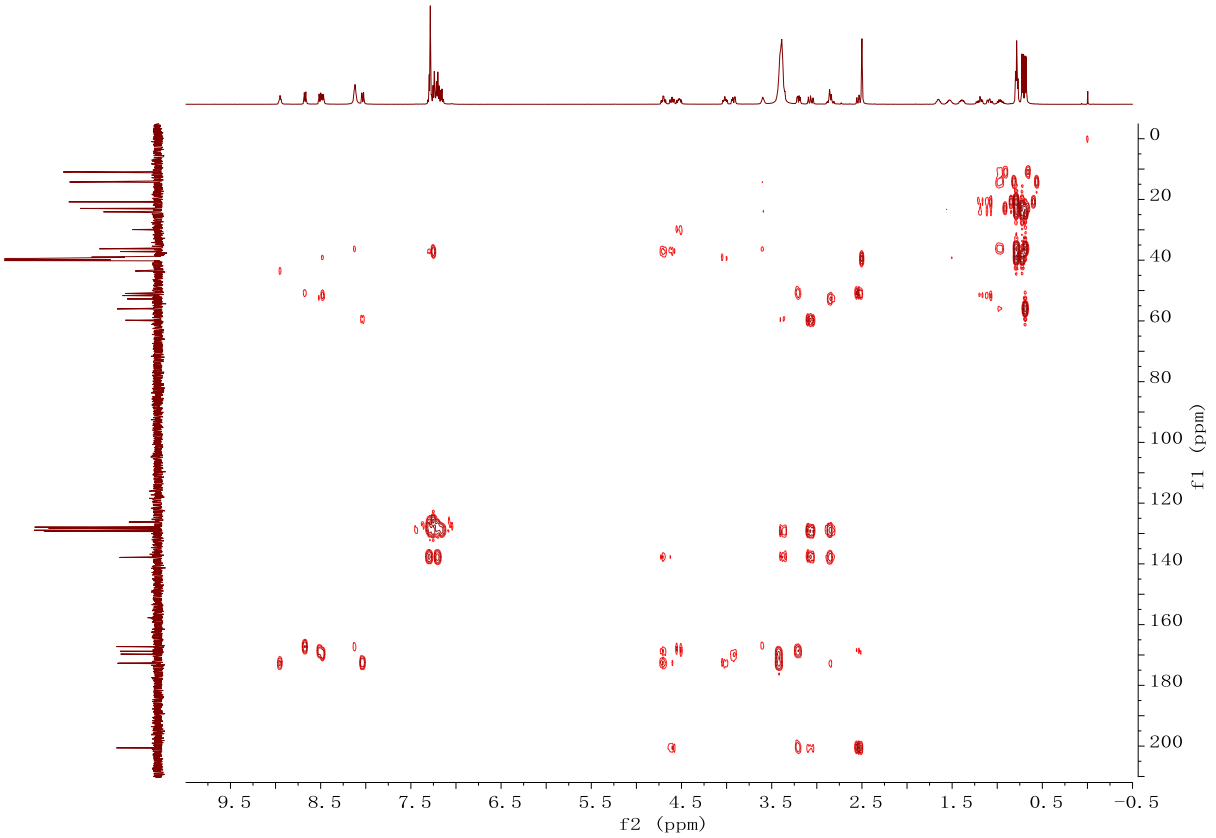

Figure S17. HMBC NMR spectrum of Pp-AIP2 (**2**) (600 MHz, DMSO-d_6).

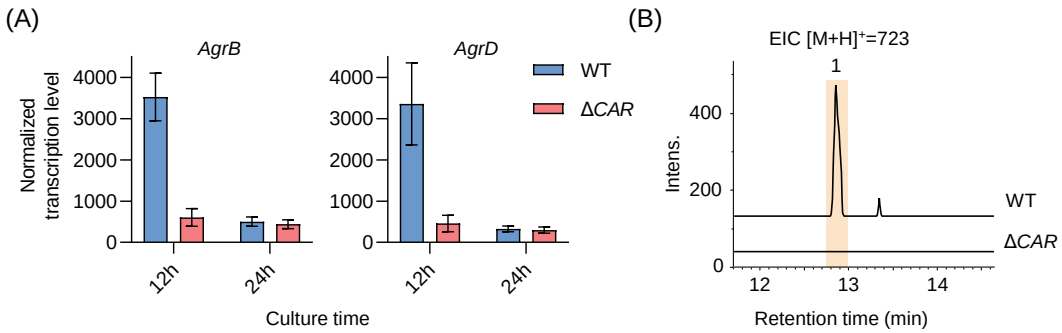

Figure S18. Expression changes of Pp-AIPs encoding genes in Δ*CAR* compared to WT.
(A) The transcription level of gene *agrB* and *agrD* in WT and Δ*CAR* strains.
(B) Extracted ion chromatograms (EICs) of Pp-AIP1 (**1**) in WT and Δ*CAR* strains.

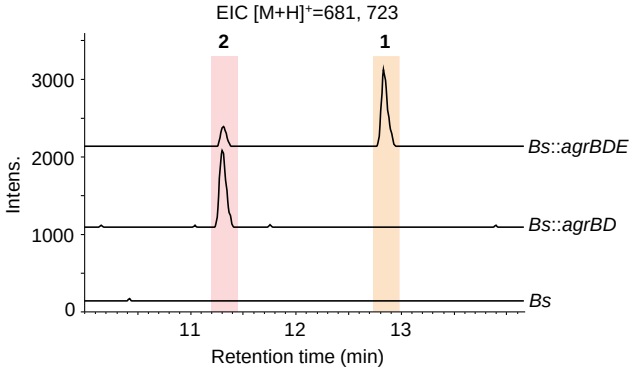

Figure S19. EICs of Pp-AIP1 (**1**) and Pp-AIP2 (**2**) in *B. subtilis* heterologous expression strains. The EICs of Pp-AIP1 (1) and Pp-AIP2 (2) in *B. subtilis* 168::*agrBDE* (*Bs*::*agrBDE*) and *B. subtilis* 168::*agrBD* (*Bs*::*agrBD*) were analyzed, with host *B. subtilis* 168 (*Bs*) as control.

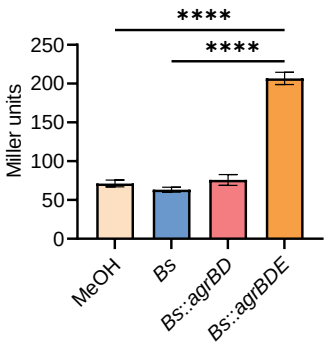

Figure S20. The lacZ activity of reporter strain in the presence of extracts from *B*. *subtilis* 168 (*Bs*), *B*. *subtilis* 168::*agrBD* (*Bs*::*agrBD*) and *B*. *subtilis* 168::*agrBDE* (*Bs*::*agrBDE*).

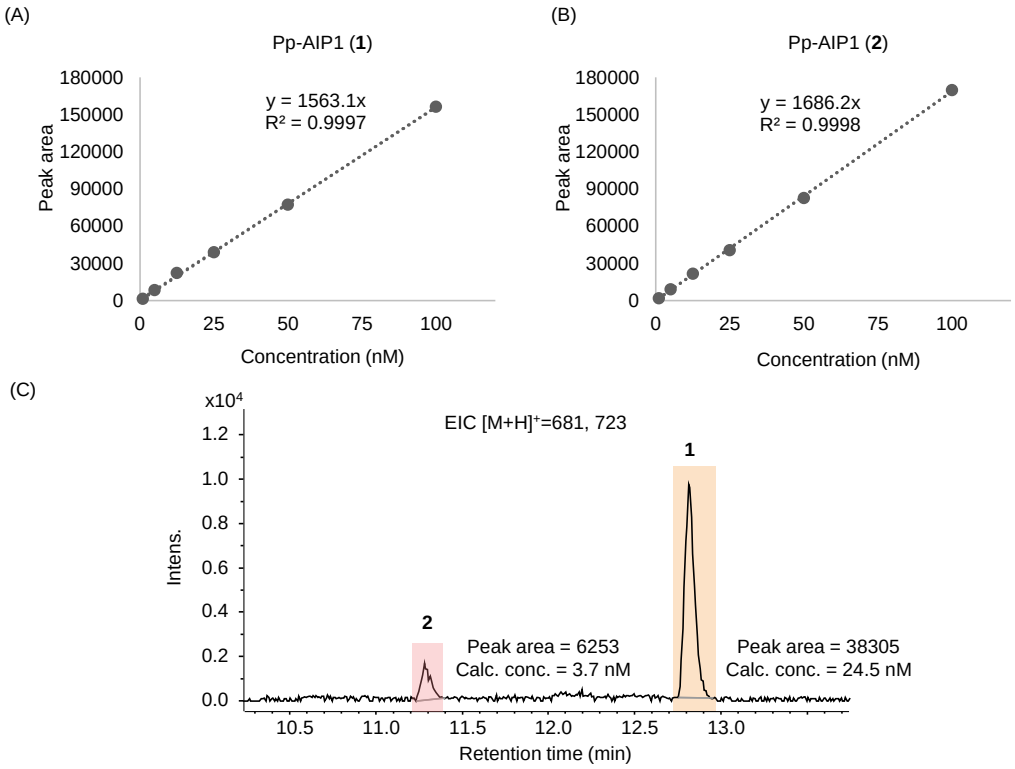

Figure S21. The quantitative measurement of the natural product concentrations of Pp-AIP1 and Pp-AIP2.

(A) The standard curve of gradient concentrations of Pp-AIP1 measured using UPLC-MS.

(B) The standard curve of gradient concentrations of Pp-AIP2 measured using UPLC-MS.

(C) The measurement of natural product Pp-AIP1 and Pp-AIP2 concentrations using UPLC-MS.

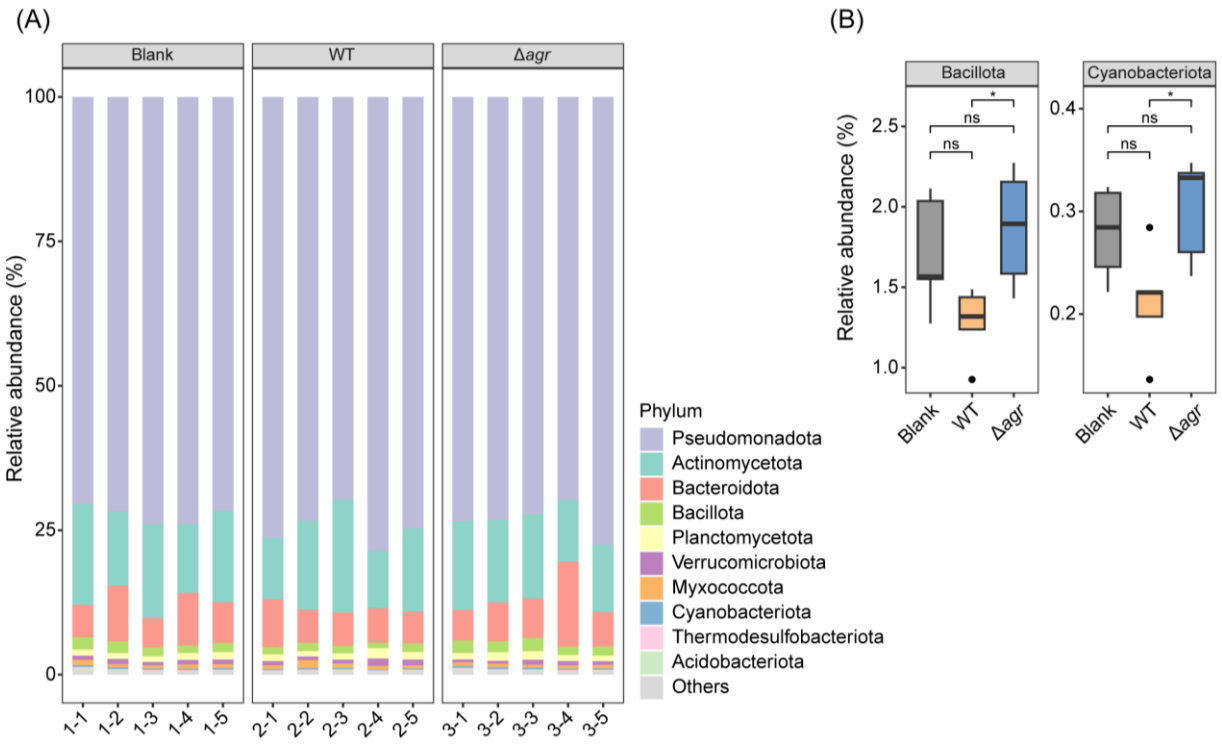

Figure S22. Effects of Pp-AIPs on the phylum level of root microbiome.

(A) Relative abundance of root bacterial phylum in each group after inoculation.

(B) The two phyla with significantly different abundances between WT and Δ*agr* group.

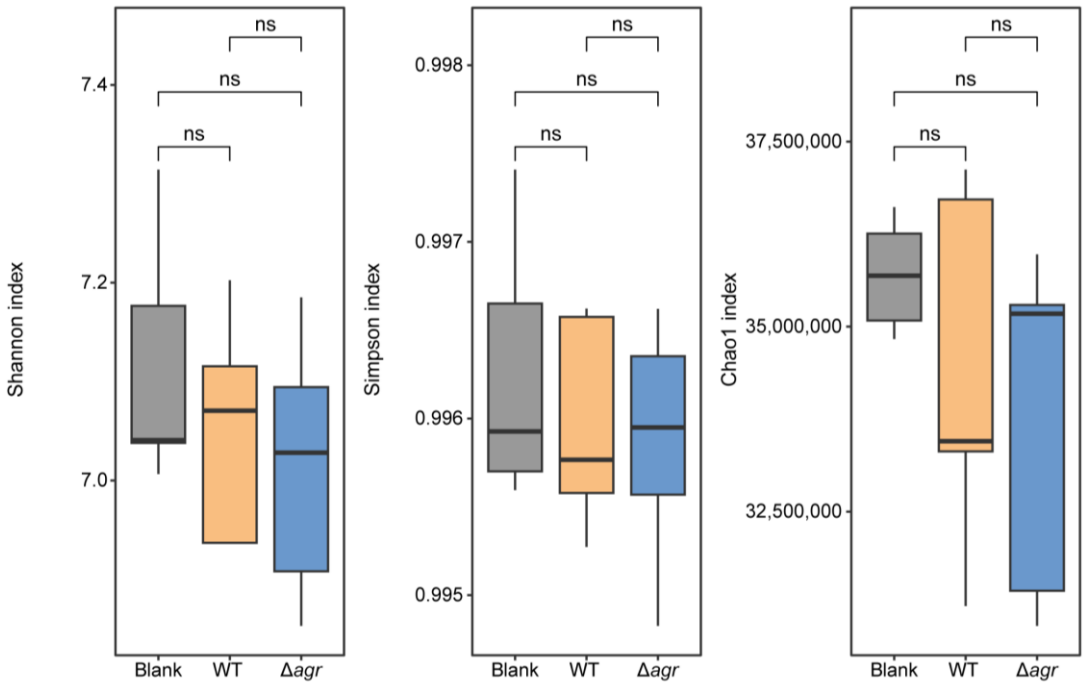

Figure S23. Alpha diversity (Shannon index, Simpson index, and Chao1 index) of root samples in response to *P. polymyxa* WT and Δ*agr* cultures.

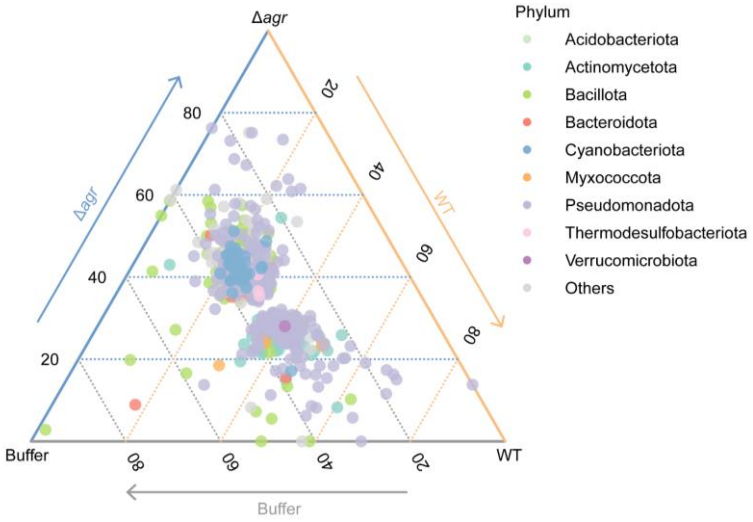

Figure S24. Ternary plots of all species with significantly different abundances in each phylum. Each dot represents one species. The position of each dot is determined by the contribution of the indicated compartments to the total relative abundance.

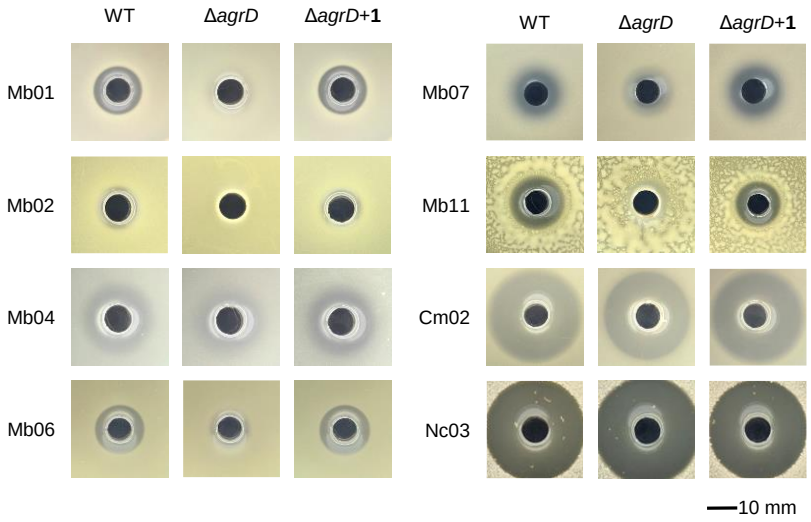

Figure S25. The effect of *agrD* inactivation (Δ*agrD*) and Pp-AIP1 supplementation (Δ*agrD*+**1**) on the antibacterial activity against 5 isolates from the root microbiome.

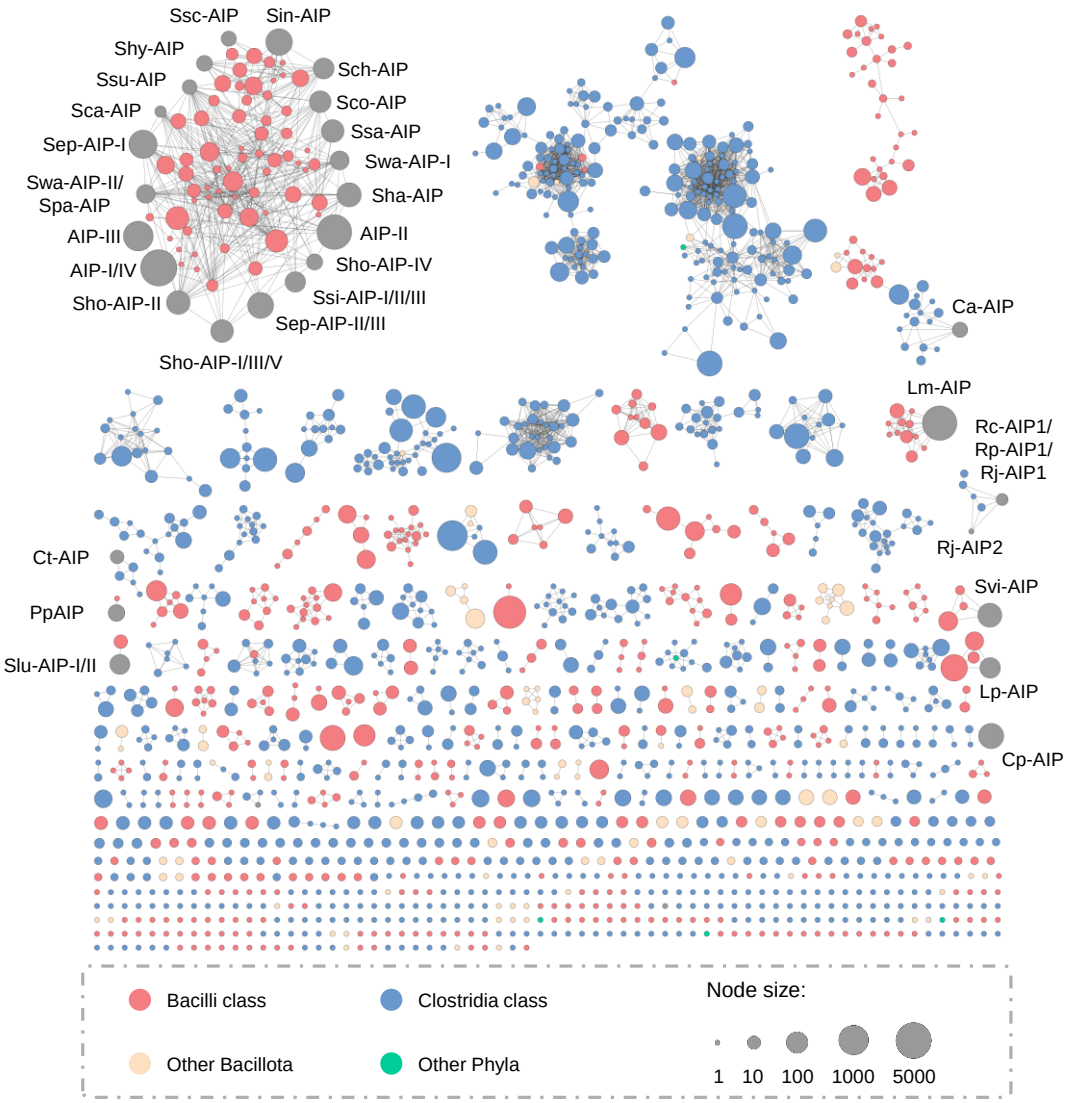

Figure S26. Sequence similarity network (SSN) of AgrDs identified by antiSMASH and TriRipp. The sequence similarity of identified AgrDs is clustered based on a 50% sequence identity threshold, with sequences sharing 80% identity are grouped into a single node. The nodes shaded in rose-color, pastel-blue and light-yellow signify AgrD sequences sourced from genomes within the Bacilli class, Clostridia class and other classes of the Bacillota phylum, respectively. The nodes in mint-green represent AgrD sequences from genomes of other phyla. The node size represents the number of sequences in one node. Reported AIPs are marked as grey nodes.

Supplementary tables

Table S1. NMR data of synthetic Pp-AIP1 (**1**) (DMSO-*d6*).

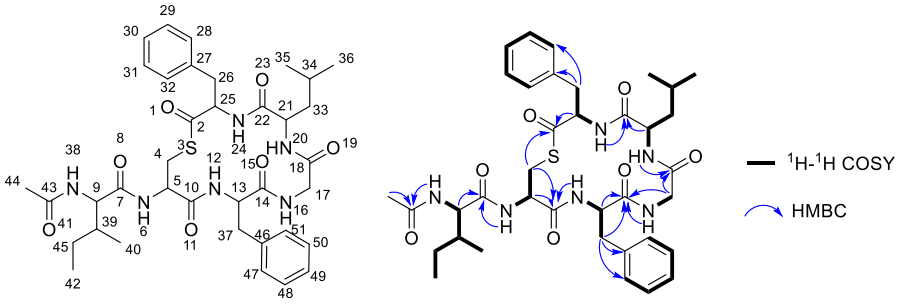

Structure of Pp-AIP1 (**1**) with the NMR assignments.

Position	δ_C	δ_H (mult, *J* [Hz])	Position	δ_C	δ_H (mult, *J* [Hz])
1-O			26	36.87	3.04 (dd, [14.3, 11.6]), 3.35 (m, overlap)
2	200.51		27	137.73	
3-S			28	129.26	7.29 (m)
4	29.8	2.61 (dd, [12.9, 10.7]), 3.13 (dd, [12.9, 5.1])	29	128.19	7.24 (m)
5	50.91	4.42 (ddd, [10.8, 8.1, 5.1])	30	126.26	7.21 (m)
6-N		8.12 (d, [8.1])	31	128.19	7.24 (m)
7	170.73		32	129.26	7.29 (m)
8-O			33	39.25	1.09 (ddd, [13.7, 10.8, 4.8]), 1.19 (ddd, [13.8, 9.6, 4.4])
9	56.44	4.16 (dd, [8.8, 7.5]	34	24.01	1.50 (m)
10	169.19		35	20.90	0.72 (d, [6.6])
11-O			36	22.90	0.78 (d, [6.7])
12-N		8.34 (d, [9.3])	37	37.04	2.86 (d, [8.2])
13	52.79	4.65 (td, [8.6, 6.4])	38-N		7.87 (d, [8.9])
14	172.55		39	36.87	1.59 (m)
15-O			40	15.18	0.65 (d, [6.8])
16-N		8.78 (t, [5.5])	41	24.45	1.00 (ddd, [13.3, 8.9, 7.1]), 1.34 (m, overlap)
17	43.47	3.39 (m, overlap), 3.88 (dd, [14.1, 4.7])	42	11.03	0.76 (t, [7.4])
18	169.50		43	169.03	
19-O			44	22.51	1.85 (s)
20-N		8.39 (d, [7.7])	45-O		
21	51.72	4.01 (ddd, [11.7, 7.7, 4.4])	46	137.83	
22	172.52		47	128.96	7.29 (m)
23-O			48	127.96	7.24 (m)
24-N		8.03 (d, [9.5])	49	126.17	7.21 (m)
25	59.68	4.60 (m)	50	127.96	7.24 (m)
			51	128.96	7.29 (m)

Table S2. NMR data of synthetic Pp-AIP2 (**2**) (DMSO-*d6*).

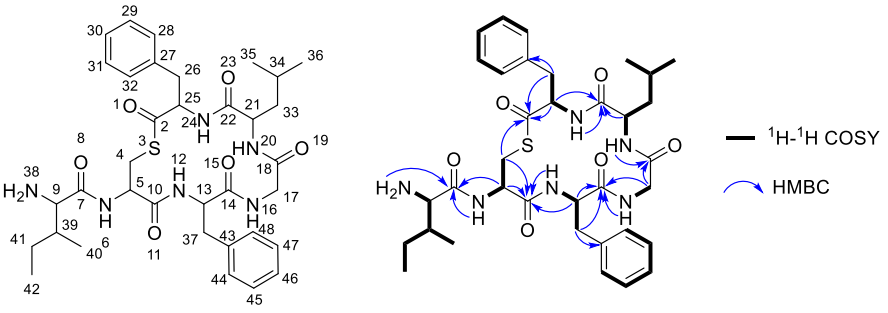

Structure of Pp-AIP2 (**2**) with the NMR assignments.

Position	δ_C	δ_H (mult, *J* [Hz])	Position	δ_C	δ_H (mult, *J* [Hz])
1-O			25	59.77	4.61 (ddd, [11.8, 9.5, 3.5])
2	200.58		26	37.15	3.07 (dd, [14.2, 11.8]), 3.37 (m, overlap)
3-S			27	137.68	
4	29.92	2.54 (m, overlap), 3.20 (dd, [12.8, 5.2])	28	129.27	7.29 (m)
5	50.96	4.53 (ddd, [11.1, 8.5, 5.3])	29	128.24	7.21 (m)
6-N		8.67 (d, [8.5])	30	126.31	7.16 (m)
7	167.22		31	128.24	7.21 (m)
8-O			32	129.27	7.29 (m)
9	56.04	3.60 (t, [5.6])	33	39.2	1.08 (ddd, [13.7, 11.1, 4.7]), 1.19 (ddd, [13.8, 9.7, 4.2])
10	168.78		34	24.02	1.53 (m)
11-O			35	22.96	0.8 (d, overlap)
12-N		8.51 (d, [9.4])	36	20.8	0.72 (d, [6.5])
13	52.76	4.70 (td, [9.6, 5.1])	37	37.15	2.86 (m)
14	172.75		38-N		8.12 (s)
15-O			39	36.25	1.65 (m)
16-N		8.95 (t, [5.6])	40	14.27	0.69 (d, [6.9])
17	43.56	3.42 (m, overlap), 3.92 (dd, [14.0, 4.6])	41	24.08	0.97 (m), 1.39 (m)
18	169.71		42	10.96	0.78 (dd, overlap)
19-O			43	137.88	
20-N		8.48 (d, [7.7])	44	128.93	7.29 (m)
21	51.66	4.02 (ddd, [11.6, 7.7, 4.1])	45	127.89	7.21 (m)
22	172.59		46	126.13	7.16 (m)
23-O			47	127.89	7.21 (m)
24-N		8.03 (d, [9.5])	48	128.93	7.29 (m)

Table S3. The gene information of *CAR* and *agr* BGC in this study.

Gene Name	Gene annotation	Genome
CAR	CUU60_RS26345	NZ_CP024795
agrB	CUU60_RS20990	
agrD	unannotated	
agrC	CUU60_RS20995	
agrA	CUU60_RS21000	
agrE	CUU60_RS21005	

Table S4. Reported AIPs and their functions.

Class	Order	Family	Host	Name	Structure	Ecology Function	Reference
Bacilli	Bacillales	Staphylococcaceae	*Staphylococcus aureus*	AIP-I	YST-[CDFIM]	Virulence production	1
			Staphylococcus aureus	AIP-II	GVNA-[CSSLF]		
			Staphylococcus aureus	AIP-III	IN-[CDFLL]		
			Staphylococcus aureus	AIP-IV	YST-[CYFIM]		
			Staphylococcus epidermidis ATCC 12228	Sep-AIP-I	DSV-[CASYF]	Biofilm	2,3
			Staphylococcus epidermidis 1457	Sep-AIP-II	NASKYNP[CSNYL]		
			Staphylococcus epidermidis 8099	Sep-AIP-III	NAAKYNP[CASYL]		
			Staphylococcus lugdunensis	Slu-AIP-I	DI-[CNAYF]		4
			Staphylococcus saprophyticus (human nose isolate)	Ssa-AIP	INP-[CFGYT]	Inhibit quorum sensing in *S. aureus* *	5
			Staphylococcus lugdunensis ID A1	Slu-AIP-II	DM-[CNGYF]		
			Staphylococcus schleiferi ID 30743	Ssc-AIP	KYPF-[CIGYF]		
			Staphylococcus simulans (pig nose isolate)	Ssi-AIP	KYNP-[CLGFL]		
			Staphylococcus hyicus (pig nose isolate)	Shy-AIP	KINP-[CTVFF]		
			Staphylococcus chromogenes (pig nose isolate)	Sch-AIP	SINP-[CTGFF]		
			Staphylococcus warneri ID 5811483	Swa-AIP-I	YSP-[CTNFF]		
			Staphylococcus vitulinus ID 62	Svi-AIP	VIRG-[CTAFL]		
			Staphylococcus haemolyticus ID1312	Sha-AIP	SFTP-[CTTYF]		
			Staphylococcus hominis ID 9525	Sho-AIP-III	TYST-[CYGYF]		6
			Staphylococcus simulans	Ssi-AIP-II	KYYP-[CWGYF]		
			Staphylococcus simulans	Ssi-AIP-III	KYNP-[CWGYF]		7
			Staphylococcus hominis C5 clinical isolate	Sho-AIP-I	SYNV-[CGGYF]		
			Staphylococcus hominis	Sho-AIP-II	SYSP-[CATYF]		8
			Staphylococcus hominis	Sho-AIP-IV	TINT-[CGGYF]		
			Staphylococcus hominis	Sho-AIP-V	SQTV-[CSGYF]		
			Staphylococcus warneri	Swa-AIP-II	ANP[CAMFY]		9
			Staphylococcus caprae DSMZ 20608	Sca-AIP	YST[CSYYF]		10
			Staphylococcus pasteuri	Spa-AIP	ANP[CAGYF]		
			Staphylococcus succinus	Ssu-AIP	ATAGALP[CGGFF]		11
			Staphylococcus cohnii	Sco-AIP	TISSVKP[CTGFV]		
			Staphylococcus intermedius RN9423	Sin-AIP	RIPT[STGFF]	Hemolytic activities	12,13
		Listeriaceae	*Listeria monocytogenes* LS1	Lm-AIP	A[CFMFV]	NA	14
			Listeria monocytogenes EGD-e	Lm-AIP	[CFMFV]	Biofilm and virulence	15–18
	Lactobacillales	Lactobacillaceae	*Lactiplantibacillus plantarum* WCFS1	Lp-AIP	[CVGIW]	Adhering to surfaces	16,19
		Enterococcaceae	*Enterococcus faecalis* AH3335	Ef-AIP	QN[SPNIFGQWM]	Virulence production	20

(next page)

Class	Order	Family	Host	Name	Structure	Ecology Function	Reference
Clostridia	Eubacteriales	Clostridiaceae	*Clostridium thermocellum* DSM 1313	Ct-AIP	[SFFIF]	Growth rate	[21]
			Clostridium perfringens CN3685	Cp-AIP	[CLWFT]	Virulence production	[16,22]
			Clostridium acetobutylicum DSM 792	Ca-AIP	[CVLVTL]	Sporulation and granulose formation[23]	
			Clostridium cellulovorans DSM 3052	Cc-AIP1	[CVTAL]	NA	
		Lachnospiraceae	*Ruminiclostridium cellulolyticum* DSM 5812	Rc-AIP1	[CWFWSY]	Endospore formation	[24]
			Ruminiclostridium papyrosolvens DSM 2782	Rp-AIP1	[CWFWSY]	NA	
			Ruminiclostridium papyrosolvens DSM 2782	Rp-AIP2	[CFLWG]	NA	
			Ruminiclostridium josui DSM 25723	Rj-AIP1	[CWFWSY]	NA	
			Ruminiclostridium josui DSM 25723	Rj-AIP2	[CWMFSF]	NA	

(last page)

* In vitro experiments using *S. aureus* RN10829 reporter strains to evaluate the QS-inhibition activity.

The structures filled with yellow represent cyclic lactones, filled with green represent exotail-free cyclic thiodepsipeptides, and not filled with color represent thiodepsipeptides with exotails.

Table S5. The effect of *agrD* inactivation (Δ*agrD*) on the antibacterial activity against isolated root-associated microbes.

Isolate	Family	Top-hit taxon	Average diameter (mm)	
			WT	Δ*agrD*
Mb01	Microbacteriaceae	*Microbacterium paraoxydans*	16.1	11.7
Mb02	Microbacteriaceae	*Microbacterium paraoxydans*	12.6	9.1
Mb03	Microbacteriaceae	*Microbacterium foliorum*	15.0	9.5
Mb04	Microbacteriaceae	*Microbacterium azadirachtae*	14.8	13.3
Mb05	Microbacteriaceae	*Microbacterium hydrocarbonoxydans*	9.5	8.6
Mb06	Microbacteriaceae	*Microbacterium hydrocarbonoxydans*	15.4	10.8
Mb07	Microbacteriaceae	*Microbacterium trichothecenolyticum*	25.7	15.7
Mb08	Microbacteriaceae	*Microbacterium jejuense*	22.4	23.6
Mb09	Microbacteriaceae	*Microbacterium jejuense*	22.0	16.4
Mb10	Microbacteriaceae	*Leifsonia soli*	18.9	18.0
Mb11	Microbacteriaceae	*Leifsonia soli*	18.9	11.9
Cm01	Cellulomonadaceae	*Cellulomonas humilata*	24.9	14.2
Cm02	Cellulomonadaceae	*Cellulomonas humilata*	32.7	27.7
Mc01	Micrococcaceae	*Arthrobacter pascens*	21.8	22.7
Nc01	Nocardioidaceae	*Aeromicrobium lacus*	28.2	27.6
Nc02	Nocardioidaceae	*Nocardioides simplex*	19.4	19.1
Nc03	Nocardioidaceae	*Nocardioides albus*	23.3	25.9
Nc04	Nocardioidaceae	*Nocardioides ultimimeridianus*	31.6	31.8
Gd01	Gordoniaceae	*Williamsia serinedens*	29.0	31.8
Gd02	Gordoniaceae	*Williamsia serinedens*	23.5	23.6
Gd03	Gordoniaceae	*Gordonia soli*	19.3	21.3
Gd04	Gordoniaceae	*Gordonia soli*	26.0	26.5
Pb01	Phyllobacteriaceae	*Mesorhizobium amorphae*	14.4	14.5
Eb01	Enterobacteriaceae	*Enterobacter cancerogenus*	15.1	14.2
Pm01	Pseudomonadaceae	*Pseudomonas crudilactis*	16.3	16.1
Pm02	Pseudomonadaceae	*Pseudomonas putida*	14.3	14.4
Pm03	Pseudomonadaceae	*Pseudomonas glycinae*	14.0	13.7
Bk01	Burkholderiaceae	*Ralstonia insidiosa*	10.3	9.8
Bk02	Burkholderiaceae	*Cupriavidus agavae*	20.3	20.0
Rb01	Rhodanobacteraceae	*Luteibacter aegosomaticola*	20.8	21.8
Lb01	Lysobacteraceae	*Stenotrophomonas panacihumi*	20.3	20.5
Lb02	Lysobacteraceae	*Stenotrophomonas bentonitica*	19.1	18.9
Lb03	Lysobacteraceae	*Stenotrophomonas maltophilia*	16.0	16.1
Lb04	Lysobacteraceae	*Stenotrophomonas maltophilia*	17.2	16.6

Lb05	Lysobacteraceae	*Lysobacter auxotrophicus*	25.2	24.9
Lb06	Lysobacteraceae	*Lysobacter soli*	24.0	24.0
Lb07	Lysobacteraceae	*Lysobacter niastensis*	23.8	25.3
Lb08	Lysobacteraceae	*Lysobacter niabensis*	26.2	26.0
Lb09	Lysobacteraceae	*Lysobacter panacisoli*	25.0	24.0
Lb10	Lysobacteraceae	*Lysobacter panacisoli*	24.0	23.2
Lb11	Lysobacteraceae	*Lysobacter prati*	24.9	24.2
Lb12	Lysobacteraceae	*Lysobacter prati*	26.7	26.5
Lb13	Lysobacteraceae	*Lysobacter prati*	24.7	24.5

Table S6. Strains used in this study.

Strains	Description	Source
E.coli DH5α	Cloning host	Lab Stock
Paenibacillus polymyxa ATCC 842	Wildtype strain	Lab stock
P. polymyxa ATCC 842 Δ*CAR*	*P. polymyxa* ATCC 842 with 3600 bp deletion for inactivating the *PpCAR* gene	Lab Stock
P. polymyxa ATCC 842 Δ*agr*	*P. polymyxa* ATCC 842 with 1623 bp deletion for inactivating the *agrBDC* gene	This study
P. polymyxa ATCC 842 Δ*agrE*	*P. polymyxa* ATCC 842 with 742 bp deletion for inactivating the *agrE* gene	This study
P. polymyxa ATCC 842 Δ*agrD*	*P. polymyxa* ATCC 842 with 106 bp deletion for inactivating the *agrD* gene	This study
P. polymyxa ATCC 842 P*pae*-lacZ	*P. polymyxa* ATCC 842 containing the plasmid pJOE8999-P*pae*-lacZ	This study
Bacillus subtilis 168	Host strain for heterologous expression	Lab stock
B.subtilis 168::*agrBD*	Heterologous expression strain of the *agrBD* genes	This study
B.subtilis 168::*agrBD*E	Heterologous expression strain of the *agrBDE* genes	This study

Table S7. Plasmids used in this study.

Plasmids	Description	Source
pDR111	The recombinant plasmid for the gene expression in *B. subtilis* 168, ampicillin resistant in *E.coli* DH5α and spectinomycin resistant in *B. subtilis* JH642	Lab Stock
pJOE8999	The plasmid for gene deletion in *P. polymyxa* ATCC 842, kanamycin resistant in *E.coli* DH5α, and *P. polymyxa* ATCC 842	Lab Stock
pJOE8999-*agr*	The plasmid for inactivating *agrBDC* in *P. polymyxa* ATCC 842	This study
pJOE8999-*agrE*	The plasmid for inactivating *agrE* in *P. polymyxa* ATCC 842	This study
pJOE8999-*agrD*	The plasmid for inactivating *agrD* in *P. polymyxa* ATCC 842	This study
pDR111-*agrBD*	The plasmid for heterologous expression of *agrBD*	This study
pDR111-*agrBDE*	The plasmid for heterologous expression of *agrBDE*	This study
pJOE8999-P*pae*-lacZ	The plasmid for evaluating the transcription level of the paenibacillin precursor gene	This study

Table S8. Primers used in this study.

No.	Primer	Sequence 5'→3'	Description
For the construction of the promoter-reporter system in *P. polymyxa*			
01	pJOE8999-F	GGCCATGACCAAAATCCCTT	Amplify the backbone from pJOE8999 plasmid for the construction of pJOE8999-Ppae-lacZ .
02	pJOE8999-R	GGTACATTTTACTCAATTCTCTAATCACG	
03	Ppae-F	aagggattttggtcatggccAAAGATGGGGATCGGGTCAA	Amplify the putative promoter region of the precursor gene in paenibacillin BGC from *P. polymyxa* ATCC 842.
04	Ppae-R	catggtcatTTTCCTCTTCCTCTCTAAATTAAATTCTA	
05	lacZ-F	ggaagaggaaaATGACCATGATTACGGATTCACTG	Amplify the *lacZ* gene from *E. coli* Trans5α.
06	lacZ-R	agaattgagtaaaatgtaccTTATTTTTGACACCAGACCAACTGG	
For the construction of vectors for genetic manipulation in *P. polymyxa*			
01	dagr-UP-F	AAGGCCAACGAGGCCatgcggctcttgatacagtagg	Amplify the homologous fragments of *agr* locus.
02	dagr-UP-R	AAGGCCATGTTGGCCcctccctaacttaattgtgcgg	
03	dagr-DOWN-F	AAGGCCAACATGGCCgatcatcggactaggactgattatc	
04	dagr-DOWN-R	AAGGCCTTATTGGCCtatcgtcttcatggatcagcac	
05	dagr-sgRNA-F	ggcataactccttctcattaGTTTTAGAGCTAGAAATAGCAAGTTAAAAT	Insert the gRNA fragment for *agr* locus by Gibson assembly.
06	dagr-sgRNA-R	taatgagaaggagttatgccCGTAGGTACATTTTACTCAATTCTCT	
07	dagrE-UP-F	AAGGCCAACGAGGCCagcctgtgttggatgtcaat	Amplify the homologous fragments of *agrE* gene.
08	dagrE-UP-R	AAGGCCATGTTGGCCcgaagaactatgccctccgt	
09	dagrE-DOWN-F	AAGGCCAACATGGCCtctgctgaagttggctattgatt	
10	dagrE-DOWN-R	AAGGCCTTATTGGCCctttgctacttcttccggct	
11	dagrE-sgRNA-F	acaatgcgccttgctctaacGTTTTAGAGCTAGAAATAGCAAGTTAAAAT	Insert the gRNA fragment for *agrE* gene by Gibson assembly.
12	dagrE-sgRNA-R	gttagagcaaggcgcattgtCGTAGGTACATTTTACTCAATTCTCT	
13	dagrD-UP-F	AAGGCCAACGAGGCCcgatgctgctttcctatacag	Amplify the homologous fragments of *agrD* gene.
14	dagrD-UP-R	AAGGCCATGTTGGCCctttaatattcttgatattgttcataattggca	

15	dagrD-DOWN-F	AAGGCCAACATGGCCaacccaaaagtttggaaattgaaca	
16	dagrD-DOWN-R	AAGGCCTTATTGGCCtgaagatggtaaggatggcg	
17	dagrD-sgRNA-F	agtaaaagaggtgaaggaggGTTTTAGAGCTAGAAATAGCAAGTTAAAAT	Insert the gRNA fragment for *agrD* gene by Gibson assembly.
18	dagrD-sgRNA-R	cctccttcacctcttttactCGTAGGTACATTTTACTCAATTCTCT	
For the validation of genetic manipulation in *P. polymyxa*			
01	dagr-Check-F	gcaggatagtgacttactggtagg	Validation of *agr* locus deletion in *P. polymyxa* ATCC 842.
02	dagr-Check-R	cgattgtccgctttcgttga	
03	dagrE-Check-F	ggttgtcagatgaagggactgg	Validation of *agrE* gene deletion in *P. polymyxa* ATCC 842.
04	dagrE-Check-R	tggaaacgccaaaatgccgt	
05	dagrD-Check-F	catggccatcgcactagatt	Validation of *agrD* gene deletion in *P. polymyxa* ATCC 842.
06	dagrD-Check-R	cttagaccattgccgctgac	
For the construction of heterologous expression plasmids in *B. subtilis*			
01	pDR111-F	AGCTTAATTGTTATCCGCTCACAAT	Amplify the backbone from pDR111 plasmid for the construction of pDR111-*agrBD(E)*.
02	pDR111-R	CGCATGCAAGCTAATTCGGTGGAAA	
03	agr-F	GAGCGGATAACAATTAAGCTggaggggcggtggcgttgta	Amplify the gene sequence of *agrBD* from *P. polymyxa* ATCC 842.
04	agr-R	TTTCCACCGAATTAGCTTGCATGCGtcatttttgttcaatttccaaacttttgggt	
03	agr-F	GAGCGGATAACAATTAAGCTggaggggcggtggcgttgta	Amplify the gene sequence of *agrBD* from *P. polymyxa* ATCC 842, which could be assembled with the *agrE* PCR fragment.
05	agr-R-agrE	gaagaactattcatttttgttcaatttccaaacttttgggt	
06	agrE-F	ttgaacaaaaaatgaatagttcttcgggaagaaaagggga	Amplify the gene sequence of *agrE* from *P. polymyxa* ATCC 842.
07	agrE-R	ACCGAATTAGCTTGCATGCGttatatgtaataatcaatagccaacttcagca	

References

1. Wang, B. & Muir, T. W. Regulation of Virulence in Staphylococcus aureus: Molecular Mechanisms and Remaining Puzzles. *Cell Chemical Biology* **23**, 214–224 (2016).

2. Olson, M. E. *et al.* Staphylococcus epidermidis agr Quorum-Sensing System: Signal Identification, Cross Talk, and Importance in Colonization. *Journal of Bacteriology* **196**, 3482–3493 (2014).

3. Vuong, C., Gerke, C., Somerville, G. A., Fischer, E. R. & Otto, M. Quorum-Sensing Control of Biofilm Factors in Staphylococcus epidermidis. *The Journal of Infectious Diseases* **188**, 706–718 (2003).

4. Tal-Gan, Y., Ivancic, M., Cornilescu, G. & Blackwell, H. E. Characterization of structural elements in native autoinducing peptides and non-native analogues that permit the differential modulation of AgrC-type quorum sensing receptors in Staphylococcus aureus. *Org. Biomol. Chem.* **14**, 113–121 (2015).

5. Gless, B. H. *et al.* Identification of autoinducing thiodepsipeptides from staphylococci enabled by native chemical ligation. *Nat. Chem.* **11**, 463–469 (2019).

6. Brown, M. M. *et al.* Novel Peptide from Commensal Staphylococcus simulans Blocks Methicillin-Resistant Staphylococcus aureus Quorum Sensing and Protects Host Skin from Damage. *Antimicrobial Agents and Chemotherapy* **64**, 10.1128/aac.00172-20 (2020).

7. Williams, M. R. *et al.* Quorum sensing between bacterial species on the skin protects against epidermal injury in atopic dermatitis. *Science Translational Medicine* **11**, eaat8329 (2019).

8. Severn, M. M. *et al.* The Ubiquitous Human Skin Commensal Staphylococcus hominis Protects against Opportunistic Pathogens. *mBio* **13**, e00930-22 (2022).

9. Severn, M. M. *et al.* The Commensal *Staphylococcus warneri* Makes Peptide Inhibitors of MRSA Quorum Sensing that Protect Skin from Atopic or Necrotic Damage. *Journal of Investigative Dermatology* **142**, 3349-3352.e5 (2022).

10. Paharik, A. E. *et al.* Coagulase-Negative Staphylococcal Strain Prevents Staphylococcus aureus Colonization and Skin Infection by Blocking Quorum Sensing. *Cell Host & Microbe* **22**, 746-756.e5 (2017).

11. Gless, B. H. *et al.* Chemical phylogenetics of the staphylococcal quorum sensing landscape. 2021.04.18.440348 Preprint at https://doi.org/10.1101/2021.04.18.440348 (2021).

12. Kalkum, M., Lyon, G. J. & Chait, B. T. Detection of secreted peptides by using hypothesis-driven multistage mass spectrometry. *Proceedings of the National Academy of Sciences* **100**, 2795–2800 (2003).

13. Ji, G. *et al.* Staphylococcus intermedius Produces a Functional agr Autoinducing Peptide

Containing a Cyclic Lactone. *Journal of Bacteriology* **187**, 3139–3150 (2005).

14. Todd, D. A. *et al.* Signal Biosynthesis Inhibition with Ambuic Acid as a Strategy To Target Antibiotic-Resistant Infections. *Antimicrobial Agents and Chemotherapy* **61**, 10.1128/aac.00263-17 (2017).

15. Zetzmann, M., Sánchez-Kopper, A., Waidmann, M. S., Blombach, B. & Riedel, C. U. Identification of the agr Peptide of Listeria monocytogenes. *Frontiers in Microbiology* **7**, (2016).

16. Gless, B. H. *et al.* Rearrangement of Thiodepsipeptides by S → N Acyl Shift Delivers Homodetic Autoinducing Peptides. *J. Am. Chem. Soc.* **143**, 10514–10518 (2021).

17. Riedel, C. U. *et al.* AgrD-dependent quorum sensing affects biofilm formation, invasion, virulence and global gene expression profiles in Listeria monocytogenes. *Molecular Microbiology* **71**, 1177–1189 (2009).

18. Bejder, B. S. *et al.* A short-lived peptide signal regulates cell-to-cell communication in Listeria monocytogenes. *Commun Biol* **7**, 1–11 (2024).

19. Sturme, M. H. *et al.* An agr-Like Two-Component Regulatory System in Lactobacillus plantarum Is Involved in Production of a Novel Cyclic Peptide and Regulation of Adherence. *Journal of Bacteriology* **187**, 5224–5235 (2005).

20. Nakayama, J. *et al.* Gelatinase biosynthesis-activating pheromone: a peptide lactone that mediates a quorum sensing in Enterococcus faecalis. *Molecular Microbiology* **41**, 145–154 (2001).

21. Verbeke, T. J. *et al.* Pentose sugars inhibit metabolism and increase expression of an AgrD-type cyclic pentapeptide in Clostridium thermocellum. *Sci Rep* **7**, 43355 (2017).

22. Ma, M., Li, J. & McClane, B. A. Structure-Function Analysis of Peptide Signaling in the Clostridium perfringens Agr-Like Quorum Sensing System. *Journal of Bacteriology* **197**, 1807–1818 (2015).

23. Steiner, E., Scott, J., Minton, N. P. & Winzer, K. An agr Quorum Sensing System That Regulates Granulose Formation and Sporulation in Clostridium acetobutylicum. *Applied and Environmental Microbiology* **78**, 1113–1122 (2012).

24. Molloy, E. M. *et al.* Enzyme-Primed Native Chemical Ligation Produces Autoinducing Cyclopeptides in Clostridia. *Angewandte Chemie International Edition* **60**, 10670–10679 (2021).